

Conceptual Nuclear Design of Innovative Liquid HALEU-loaded Thermal Propulsion Reactor

Reem Alnuaimi^a, and Yonghee Kim^a

^aDepartment of Nuclear & Quantum Engineering, Korea Advanced Institute of Science and Technology (KAIST), 291 Daehak-ro, Yuseong-gu, Daejeon 34141, Republic of Korea

Abstract

Crewed missions beyond low Earth orbit (LEO) require more advanced propulsion than chemical engines. The Nuclear Thermal Rocket (NTR) is a promising solution that uses nuclear reactors to heat hydrogen propellant for thrust. The melting temperature of solid fuels limits traditional NTRs. This study presents a liquid-core NTR design with High-Assay Low-Enriched Uranium (HALEU) and uranium-manganese (UMn) fuel, capable of operating up to 3500°C. This fuel enables better reactivity control and longer reactor lifetime by removing neutron-absorbing fission products. Core calculations using the Serpent 2.20 code confirmed criticality, with over 92% of fissions in the thermal/epithermal spectrum and a reactor mass of 2250 kg. Moderators such as synthetic diamond, graphite, and BeO optimize neutron moderation and performance. This concept enhances NTR performance, safety, and proliferation resistance, paving the way for future deep-space missions.

***Keywords :** Nuclear Thermal Rocket (NTR), HTGR, HALEU, Synthetic Diamond (SD)

1. Introduction

Future crewed space missions beyond low Earth orbit (LEO) will require advanced propulsion systems that surpass current chemical engines. Nuclear thermal rockets (NTR) are a promising alternative because they generate thrust through heat, similar to chemical rockets, but rely on controlled fission of uranium or other fissile materials instead of combustion [1]. NTRs can increase the specific impulse (I_{sp}) of chemical rockets to around 900 seconds by expanding a propellant thermodynamically, as shown in Figure 1, which compares chemical and nuclear rocket structures [2].

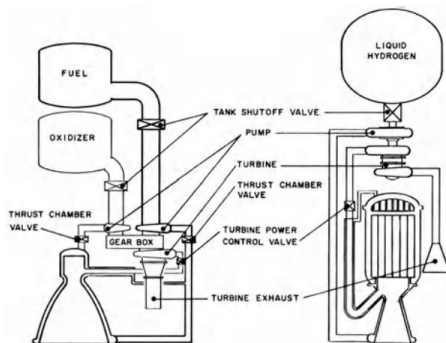


Fig. 1. Schematic comparison of chemical and nuclear rockets [3].

Solid-core nuclear reactors, such as the U.S. NERVA and Particle Bed Reactor (PBR) or the Soviet RD-410, are the only propulsion designs developed to date. These reactors typically used highly enriched uranium (HEU) and operated in the fast neutron spectrum [4]. Recent research has explored the use of low-enriched uranium (LEU), which could enhance neutron economy while improving proliferation resistance [5].

The temperature limits for fuel and structures in solid-core NTRs are around 2500 K, although research suggests this could eventually reach 3000 K. Both the U.S. and Soviet Union tested materials at up to 2500 K in the 1960s, with rockets achieving thrust levels of 450 kN. While the I_{sp} in these rockets is constrained to less than 1000 s due to propellant temperatures, this still exceeds the I_{sp} of chemical rockets by more than double. However, sustained thrust at 1000 s would deplete propellant quickly. Although this I_{sp} could shorten human missions to Mars compared to chemical propulsion, it remains insufficient for more distant missions, such as to Jupiter's moon Europa. Any future improvements in NTR propulsion would need to overcome current structural and thermodynamic limitations [2].

Liquid fuel cores are an innovative way to overcome uranium-based fuels' melting point. Based on a high-temperature gas-cooled reactor (HTGR) concept, this study examined a preliminary liquid High-Assay Low-Enriched Uranium (HALEU) Nuclear Thermal Rocket (NTR) core. The fuel used in the core is a uranium-manganese (UMn) liquid eutectic metal, with a 19.75% enrichment of U-235 and 94.05% uranium and 5.95% manganese by weight.

This fuel is liquid at a low melting point of 716 °C [6] and is capable of operating at high temperatures up to 3500 °C without boiling, which is its distinguishing property. Unlike solid fuel cores, where fissile products such as Xe-135 accumulate and reduce reactivity via neutron absorption, the liquid fuel system effectively removes such byproducts via noble gas diffusion. This not only decreases their impact on reactor performance, but also makes reactivity control easier and extends the core's lifetime.

2. Reactor Concept and Methods

2.1 General Considerations

Nuclear reactors are systems containing enough fissionable material, such as Uranium or Plutonium, to sustain a chain reaction. The energy source in these reactors comes from the excess binding energy of the fissionable material compared to that of the resulting fission products. The reaction is initiated when a fissionable atom absorbs a neutron. For the reaction to be self-sustaining, at least one neutron from each fission event must be absorbed by another fissionable nucleus, triggering further fission.

Figure 2 depicts a typical nuclear rocket reactor system. The core, made of fissionable uranium dispersed in a high-temperature matrix, acts as a heat exchanger. The core is supported by structural components attached to a support plate at the cooler end of the system, where coolant enters. A neutron reflector surrounds the core to reduce neutron losses by reflecting neutrons back into the core. Rotating drums containing neutron-absorbing material (poison) control the reactor's power. By withdrawing the poison towards the reflector's outer edge, more neutrons are reflected back into the core, increasing power. Rotating the drums inward reduces neutron reflection, decreasing power. Once the desired power level is reached, the drums are adjusted to maintain steady-state operation.

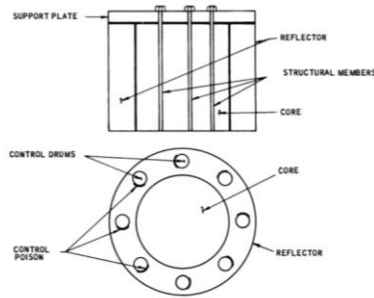


Fig. 2. Schematic of nuclear rocket reactor [3].

Core materials must withstand high temperatures in a hydrogen environment. Heat generated by fission must be efficiently removed while keeping structural components within safe temperature limits. The reactor's mechanical design ensures structural integrity, while the nuclear design guarantees a sufficient amount of fissionable material to maintain a self-sustaining chain reaction under operating conditions. Control mechanisms are essential for starting, regulating, and shutting down the reactor as needed [1].

2.2 Core Description

In this study, a reactor core consisting of 31 fuel assemblies was designed, with dimensions of 93.1 cm in both height and diameter. To mitigate neutron leakage from this compact Nuclear Thermal Rocket (NTR), a beryllium reflector with radial and top axial

thicknesses of 7 cm and 8 cm, respectively, was incorporated. Detailed cross-sectional views of the core are depicted in Figure 3.

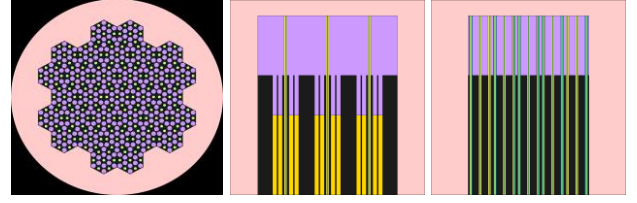


Fig. 3. Cross-sectional views of the NTR core.

The core was optimized to achieve various design objectives aimed at enhancing the performance of both the rocket and the nuclear systems. Specifically, the reactor mass was constrained to under 2500 kg to avoid unnecessary thrust consumption for spacecraft lift-off. Initially, the coolant outlet temperature, which also serves as the propellant, is set to a minimum of 3000 K to improve specific impulse. The reactor is designed to operate mainly in the thermal spectrum to improve neutron economy and proliferation resistance. Additionally, to ensure the fuel remains in the liquid phase, the axial power profile is designed to support efficient heat transfer.

2.3 Fuel

Figure 4a illustrates the structure of the fuel assembly as a hexagonal block with a flat-to-flat distance of 13.3 cm. The upper third of the core is composed of BeO blocks, while the remainder is filled with graphite. The assembly can support up to 19 channels. For this study, 7 channels are designated for fuel, and the remaining 12 positions are occupied by BeO and synthetic diamond (SD) moderators, as will be illustrated in the 3-moderator model. Figure 4b and Table I provide details on the annular cooling channel, including inner and outer hydrogen cooling.

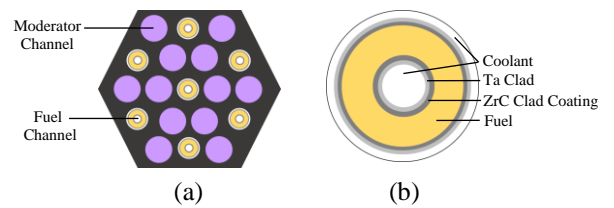


Fig. 4. Structures of a) fuel element and b) fuel channel.

Table I. Fuel channel description

| Layer | Material | Density (g/cm ³) | Outer Radius (cm) |
|--------------|----------------|------------------------------|-------------------|
| Coolant | H ₂ | 8.40E-5 | 0.118 |
| Inner Clad | Ta | 16.40 | 0.126 |
| Clad Coating | ZrC (100% TD) | 6.730 | 0.131 |
| Fuel | UMn (Liquid) | 15.29 | 0.631 |
| Clad Coating | ZrC (100% TD) | 6.730 | 0.636 |
| Outer Clad | Ta | 16.40 | 0.644 |
| Coolant | H ₂ | 8.40E-5 | 0.762 |

2.4 Moderator

To effectively utilize thermal neutrons, a moderator material capable of withstanding high temperatures must be integrated into the core matrix. Limited options are available for such materials. This study adopts a three-moderator configuration to enhance thermalization, comprising conventional graphite, BeO, and a newly explored Synthetic Diamond (SD) [7]. Recent advancements in Synthetic Diamond manufacturing have enabled diamond growth under 1 atm pressure at 1025°C, leading to potential cost reductions and significant progress in diamond synthesis [8]. While SD remains carbon-based like graphite, it offers notable advantages, including high stability at temperatures up to 3500°C, a higher carbon atom density with a theoretical mass density of 3.5 g/cm³ compared to nuclear-grade graphite's 1.7 g/cm³, and thus superior neutron slowing power and moderating efficiency.

The moderator material can be incorporated by filling either the hexagonal fuel assembly blocks, the moderator channels (1.20 cm in radius), or both. Figure 5 illustrates two options: the use of SD or its exclusion. Both configurations use BeO to fill the blocks and moderator channels in the upper one-third of the core region. The lower core is comprised of graphite-filled blocks. In the upper third of the graphite blocks, BeO fills the top portion of the moderator channels, while the remaining portion can be loaded with SD. SD channels are assumed to be partially filled with SD particles at packing factors of 70%, 75%, 80%, and 85%. Packing the SD into the channels can be achieved using a vibratory packing technique that considers geometrical parameters such as particle size distribution, shape, and surface conditions, as well as vibration variables including frequency, amplitude, and duration [7].

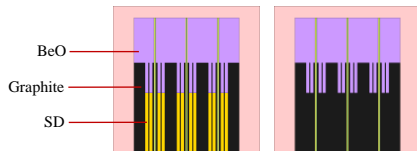


Fig. 5. The 3-moderator model.

2.5 Reactor Mass

Table II indicates the detailed mass of the core materials, while Table III shows the total mass, which is determined by whether or not SD is loaded and the packing factor used.

Table II. Mass of core materials

| Material | Mass (kg) |
|--------------------|--|
| Fuel | Total: 369.7092 (U: 347.7115/Mn: 21.9976) |
| Graphite | Without SD |
| | 400.1198 |
| With SD | 281.7417 |
| | Be (Reflector) |
| Hydrogen (Coolant) | 9.587E-04 |
| ZrC (Clad Coating) | 3.2548 |
| Ta (Clad) | 12.6904 |
| BeO | 511.4228 |

Table III. SD loading and total mass of the reactor.

| SD Packing Factor | Total SD mass (kg) | Total mass of reactor (kg) |
|-------------------|--------------------|----------------------------|
| Without SD | - | 2163.2974 |
| 70% | 170.6037 | 2215.5230 |
| 75% | 182.7897 | 2227.7090 |
| 80% | 194.9757 | 2239.8950 |
| 85% | 207.1616 | 2252.0809 |

3. Results and Analysis

In the analysis of a nuclear reactor system, the Boltzmann transport equation provides a rigorous representation of neutron behavior in terms of time, space, and energy. This equation describes how neutron flux evolves due to interactions like collisions, absorptions, and fissions. To analyze reactor behavior, the Monte Carlo method is often employed. This technique traces the paths of individual neutrons by randomly selecting their directions, energy levels, and collision paths. The Monte Carlo method is known for its precision in modeling neutron behavior and is highly effective for understanding complex reactor systems [1].

In this study, core calculations were performed using the Continuous-Energy Monte Carlo code Serpent 2.20, with 100,000 neutron histories, in 50 inactive and 200 active cycles. Cross-sections of all materials were obtained from the ENDF/B-VIII.0. Because of library limitations, the cross-sectional data were evaluated at a maximum temperature of 2500 K. Furthermore, simulations were performed using thermal scattering data from the graphite and BeO matrix, as well as the Beryllium reflector. The $S(\alpha,\beta)$ data were obtained at the maximum temperatures available in the ENDF/B-VII.0 library: 2000 K for graphite and 1200 K for Beryllium and BeO. Outside the core, vacuum boundary conditions were applied both radially and axially.

3.1 Neutronics

In nuclear reactor terminology, maintaining a sustainable fission chain reaction is described by the multiplication factor k , where it represents the ratio of the number of neutrons produced to the number of neutrons lost in each cycle. For a controllable fission chain reaction, such as in typical nuclear reactors, k should be slightly above 1, indicating a supercritical state with a controlled excess reactivity. In this study, the core's excess reactivity limit, in without SD loading case, is kept below 1000 pcm.

Table IV demonstrates the impact of SD loading on reactivity. For instance, the effective multiplication factor k_{eff} increased from (1.00697 ± 0.00069) without SD to (1.01776 ± 0.00069) with maximum SD loading. This represents an increase in reactivity of 1052 pcm. This result aligns with expectations, as the addition of SD channels enhances moderating power, which

reduces the fission reaction rates in the fast neutron spectrum, as detailed in Table V and Figure 6. Consequently, the reactor's neutron spectrum shifts predominantly towards thermal and epithermal regions, as illustrated in Figure 7.

Table IV. The multiplication factor of the core

| SD Packing Factor | k_{eff} | $\pm\sigma$ |
|-------------------|------------------|-------------|
| Without SD | 1.00697 | 0.00069 |
| 70% | 1.01449 | 0.00064 |
| 75% | 1.01344 | 0.00073 |
| 80% | 1.01553 | 0.00069 |
| 85% | 1.01776 | 0.00069 |

Table V. Energy dependence of fission reaction rate

| SD Packing Factor | Thermal | Epithermal | Fast |
|-------------------|-----------|------------|----------|
| Without SD | 46.20692% | 45.87257% | 7.92051% |
| 70% | 46.22991% | 45.94311% | 7.82698% |
| 75% | 46.30570% | 45.89380% | 7.80050% |
| 80% | 46.30679% | 45.91517% | 7.77804% |
| 85% | 46.37333% | 45.87000% | 7.75667% |

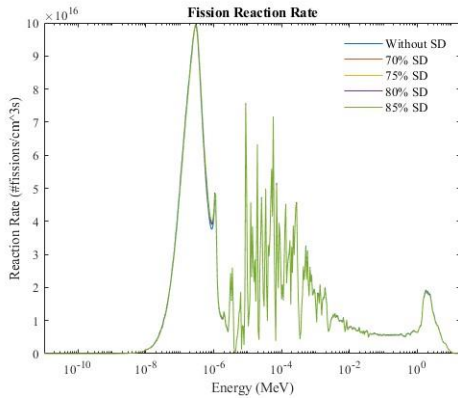


Fig. 6. Fission reaction rate spectrum.

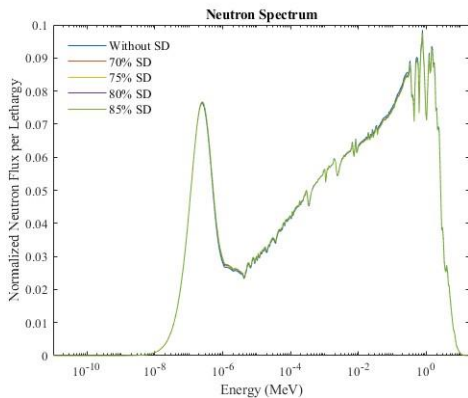


Fig. 7. Core average neutron energy spectrum.

3.2 Power Distributions

This core design is intended to generate 250 MWth. It is crucial to consider local variations in neutron flux and power distribution to avoid wasting fuel and prevent thermal hot spots. The design principle involves maintaining an axial power shape that ensures the fuel remains in a liquid state, along with achieving a radial power distribution that is as uniform as possible. Power

peaking factors are used to quantify the relative power distributions in the core, linking neutronics and thermal-hydraulics analyses. These factors help ensure that thermal power limits are satisfied. A uniform power distribution typically results in a power peaking factor value close to one.

Figure 8 depicts the axial power distribution without SD and at a maximum SD loading of 85%. The addition of SD to the lower region flattens the power peaking factor from 1.87 to 1.75, reducing fission power produced in the BeO region by 4%. The power profile was intentionally designed to keep the UMn fuel in the liquid phase. Figure 9 also analyzes the radial power distributions for the aforementioned cases, revealing power peaking factors of 1.13 and 1.14, respectively. The majority of fission power is typically generated in the middle region, because, while BeO has greater moderating power than graphite, its absorption cross section is larger. The addition of SD raises the fission power output in the lower region from 18% to 22%. Overall, power profiles are nearly flat.

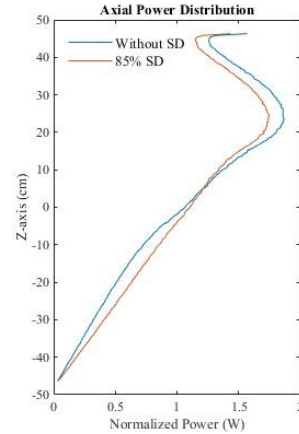


Fig. 8. Normalized axial power distribution.

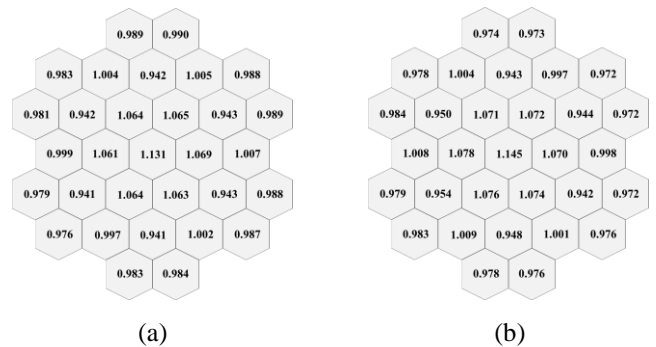


Fig. 9. Normalized radial power distributions a) without SD and b) with 85% SD loading.

3.4 Reactivity Coefficients

The neutron population in an active nuclear reactor is high enough that any change in fission heating caused

by a neutron population change will result in temperature changes, which will change k and alter reactivity or cause reactivity feedback. The temperature coefficient of reactivity (α_T) measures the difference in reactivity caused by temperature changes. The sign of α_T determines a reactor's response to temperature changes. When α_T is positive, an increase in temperature leads to an increase in the multiplication factor, which leads to an increase in the power level, resulting in a meltdown. A negative value of α_T indicates that increasing the temperature causes a decrease in power level, resulting in a return to the reactor's original state. A reactor with positive α_T is unstable to temperature changes, while a negative α_T indicates an inherently stable reactor. The fuel temperature coefficient (FTC) and the moderator temperature coefficient (MTC) are the most important reactivity coefficients in determining the reactor core's self-control.

In terms of preliminary safety analysis, the moderator, fuel, and reflector temperature coefficients were evaluated both without and with 85% SD loading at 2250 K. This calculation was performed with $S(\alpha, \beta)$ and with 6 million histories over 100 inactive and 500 active cycles, to improve accuracy. Density was adjusted to account for thermal expansion, and because the UMn fuel is liquid, volume shrinkage below the reference temperature of 2500 K was accounted for by filling the upper and lower fuel regions with void when it is denser.

As shown in Table VII, the MTC values are less negative because they incorporate the contributions of competing 3-moderator materials. For example, carbon in graphite and SD behaves generally positively, whereas BeO causes it to behave negatively, as demonstrated by the effect of loading SD into the core. FTC values are strongly negative, giving more assurance that negative feedback will override the MTC's less negative contribution. RTC values are less negative as well; however, the temperature increase in the reflector region is much smaller and slower than that in the fuel and moderator regions, so it is less concerning.

Table VII. Reactivity Coefficients at 2250 K

| | MTC [pcm/K] | | FTC [pcm/K] | | RTC [pcm/K] | |
|------------------------|-------------|---------|-------------|---------|-------------|--------|
| | NO SD | 85 SD | NO SD | 85 SD | NO SD | 85 SD |
| Reactivity Coefficient | -0.0984 | -0.0385 | -0.7550 | -0.7391 | -0.0688 | 0.0385 |
| $\pm \sigma$ | 0.0561 | 0.0555 | 0.0560 | 0.0554 | 0.0561 | 0.0707 |

4. Conclusion

In conclusion, this study introduces a novel concept for NTR technology, which addresses the limitations of solid-core designs using innovative fuel and moderator models. However, in order to fully evaluate its potential, it is necessary to model the entire reactor system, including the forward region, control mechanisms, and shielding. Furthermore, design modifications, comprehensive rocket performance, and Multiphysics analyses are required to demonstrate the NTR system's feasibility and safety.

REFERENCES

- [1] R. W. Humble, G. N. Henry and W. J. Larson, Space Propulsion Analysis and Design, The McGraw-Hill Companies, United States, 1995.
- [2] P. A. Czysz, C. Bruno and B. Chudoba, Future Spacecraft Propulsion Systems and Integration, Springer, Germany, 2018.
- [3] W. H. Loh, "Jet, Rocket, Nuclear and Electric Propulsion: Theory and Design", Springer, New York, 1968.
- [4] P. Venneri and Y. Kim, Advancements in the Development of Low Enriched Uranium Nuclear Thermal Rockets, Energy Procedia, Oct 31-Nov 2, 2016, Tokyo, Japan.
- [5] W. Emrich, Principles of Nuclear Rocket Propulsion, Elsevier, Massachusetts, 2023.
- [6] A.K. Cea, A. Leenaers, S.V. Berghe and T. Pardo, Microstructure and calorimetric analysis of the UMn binary system, Journal of Nuclear Materials, Vol.514, pp.380-392, 2019.
- [7] R. Alnuaimi, P. Venneri and Y. Kim, Feasibility of Enhancing Neutron Moderation in Nuclear Thermal Propulsion Reactor by Using Synthetic Diamond, Transactions of the American Nuclear Society, Vol. 130, pp. 1076-1079, 2024.
- [8] Y. Gong, D. Luo, M. Choe et al., Growth of diamond in liquid metal at 1 atm pressure, Nature, Vol. 629, pp.348-354, 2024.